

# Dense Feature Aggregation and Pruning for RGBT Tracking

Yabin Zhu

Key Laboratory of Intelligent Computing and Signal Processing of Ministry of Education, School of Computer Science and Technology, Anhui University  
Hefei, Anhui, China  
zhuyabin0726@foxmail.com

Chenglong Li

Key Laboratory of Intelligent Computing and Signal Processing of Ministry of Education, School of Computer Science and Technology, Anhui University  
Institute of Physical Science and Information Technology, Anhui University  
Hefei, Anhui, China  
lcl1314@foxmail.com

Bin Luo

Key Laboratory of Intelligent Computing and Signal Processing of Ministry of Education, School of Computer Science and Technology, Anhui University  
Hefei, Anhui, China  
luobin@ahu.edu.cn

Jin Tang

Key Laboratory of Intelligent Computing and Signal Processing of Ministry of Education, School of Computer Science and Technology, Anhui University  
Key Laboratory of Industrial Image Processing and Analysis of Anhui Province  
Hefei, Anhui, China  
tangjin@ahu.edu.cn

Xiao Wang

Key Laboratory of Intelligent Computing and Signal Processing of Ministry of Education, School of Computer Science and Technology, Anhui University  
Hefei, Anhui, China  
wangxiaocvpr@foxmail.com

## ABSTRACT

How to perform effective information fusion of different modalities is a core factor in boosting the performance of RGBT tracking. This paper presents a novel deep fusion algorithm based on the representations from an end-to-end trained convolutional neural network. To deploy the complementarity of features of all layers, we propose a recursive strategy to densely aggregate these features that yield robust representations of target objects in each modality. In different modalities, we propose to prune the densely aggregated features of all modalities in a collaborative way. In a specific, we employ the operations of global average pooling and weighted random selection to perform channel scoring and selection, which could remove redundant and noisy features to achieve more robust feature representation. Experimental results on two RGBT tracking benchmark datasets suggest that our tracker achieves clear state-of-the-art against other RGB and RGBT tracking methods.

## KEYWORDS

RGBT tracking, dense aggregation, recursive fusion, feature pruning

Permission to make digital or hard copies of all or part of this work for personal or classroom use is granted without fee provided that copies are not made or distributed for profit or commercial advantage and that copies bear this notice and the full citation on the first page. Copyrights for components of this work owned by others than ACM must be honored. Abstracting with credit is permitted. To copy otherwise, or republish, to post on servers or to redistribute to lists, requires prior specific permission and/or a fee. Request permissions from permissions@acm.org.

MM '19, October 21–25, 2019, Nice, France

© 2019 Association for Computing Machinery.

ACM ISBN 978-1-4503-6889-6/19/10...\$15.00

<https://doi.org/10.1145/3343031.3350928>

## ACM Reference Format:

Yabin Zhu, Chenglong Li, Bin Luo, Jin Tang, and Xiao Wang. 2019. Dense Feature Aggregation and Pruning for RGBT Tracking. In *Proceedings of the 27th ACM International Conference on Multimedia (MM'19), Oct. 21–25, 2019, Nice, France*. ACM, New York, NY, USA, 8 pages. <https://doi.org/10.1145/3343031.3350928>

## 1 INTRODUCTION

Given the initial ground truth, the task of RGBT tracking is to track a particular instance in sequential frames using RGB and thermal infrared information. Recently, it has received increasing attention as it is able to achieve robust tracking performance in challenging environments by utilizing inter-modal complementarity. Despite much progress in RGBT tracking [4, 29–31], there are still many problems need to be solved, where how to effectively fuse RGB and thermal infrared sources is a core factor in boosting tracking performance and still not solved well.

Some RGBT tracking methods [10, 11] used manual weights to achieve adaptive integration of RGB and thermal data, but their generality and scalability are low. Other methods [33, 44] performed joint sparse representation in Bayesian filtering framework by fusing features or reconstruction coefficients of different modalities. It usually introduces redundant and noisy information when some individual source is malfunction. Recently, some RGBT tracking works [24, 28] focused on introducing modality weights to achieve adaptive fusion of different source data. Lan *et al.* [24] used the max-margin principle to optimize the modality weights according to classification scores. Li *et al.* [26] employed reconstruction residues to regularize modality weight learning. However, these

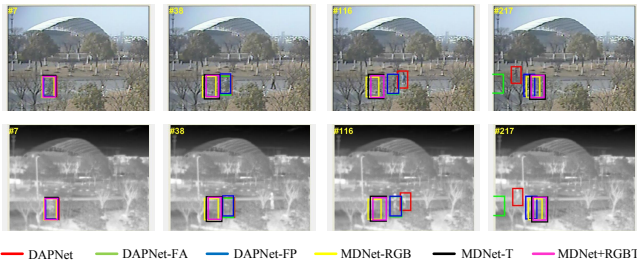


**Figure 1: Visual examples of our tracker comparing with MDNet with different inputs including RGB, thermal and RGBT, denoting MDNet-RGB, MDNet-T and MDNet+RGBT respectively. Also, we show two variants of our DAPNet, i.e., DAPNet-FA that removes feature pruning of DAPNet and DAPNet-FP that removes dense feature aggregation in DAPNet. The results demonstrate effectiveness of dense feature aggregation and feature pruning in our DAPNet.**

works would fail when the reconstruction residues or classification scores are unreliable to reflect modal reliability. The above works only rely on handcrafted feature to localize objects and thus be difficult to handle the challenges of significant appearance changes caused by deformation, background clutter and partial occlusion and low illumination within each modality. Li *et al.* [6] adopted a two-stream CNN network and a fusion network to fuse these two modalities, but they only adapted highly semantic features which are unable to locate targets precisely.

In this paper, we propose a novel approach, namely Dense feature Aggregation and Pruning Network (DAPNet), for RGBT tracking. Shallow features could encode appearance and spatial details of targets and thus are beneficial to achieving precise target localizations, while deep features are more effective to capture target semantics which can effectively identify the target category. Some existing works [25, 42] usually employ specific feature layers for sparse feature aggregation to enhance tracking performance. To make best use of deep features, our method instead recursively aggregates features of all layers in a dense fashion. As shown in Fig. 2, our DAPNet makes full use of shallow-to-deep spatial and semantic features to achieve more accurate tracking results. In addition, we also compress feature channels to reduce redundancy and use the max pooling operation to transform different sizes of feature maps into the same scale. To reduce network parameters and capture common properties of different modalities, we make RGB and thermal backbone networks sharing same parameters.

The aggregated RGBT features are noisy and redundant as some of them are useless or even interfering in locating a certain target. That is to say, only a few convolutional filters are active and a large portion of ones contain redundancy and irrelevant information in describing a certain target, which leads to over-fitting, as demonstrated in [26, 32]. To handle these problems, we propose a collaborative feature pruning method to remove noisy and redundant feature maps for more robust tracking. Existing works [18, 20] exploited reconstruction-based methods, which seek to do channel pruning by minimizing the reconstruction error of feature maps between the pruned model and a pre-trained model. However, these

methods incorrectly preserve the actual redundant channels by minimizing the reconstruction errors of the feature maps. In this paper, we apply the idea of channel pruning to solve our problem, and improve it with just simple operations to achieve excellent tracking performance.

In a specific, the feature pruning module is followed by the feature aggregation module, but it does not increase the number of network parameters and is only deployed in training phase with slight computational cost. The feature pruning module consists of two steps, *i.e.*, channel scoring and channel selection which are realized by a global average pooling and weighted random selection. Through this feature pruning method, we choose to deactivate some of the feature channels in each iteration of training, resulting in a more robust convolutional feature representation. Once the training is done, the network parameters of aggregation are fixed and feature pruning are removed during online tracking.

We validate the effectiveness of the proposed tracking framework on two RGBT tracking benchmark datasets, including GTOT [5] and RGBT234 [7]. We summarize our major contributions as follows. First, we propose a novel end-to-end trained deep network for accurate RGBT tracking. By deploying all enhanced deep features, our tracker is able to handle the challenges of significant appearance changes caused by partial occlusion, deformation and adverse environmental conditions, etc. Extensive experiments show that the proposed method outperforms other state-of-the-art trackers on RGBT tracking datasets. Second, we propose a dense feature aggregation module to recursively integrate features of all layers into a same feature space. Finally, to further eliminate effects of noisy features after dense feature aggregation, we design a feature pruning module to obtain more robust feature representation and achieve better tracking performance.

## 2 RELATED WORK

In this section, we give a brief review of tracking methods closely related to this work.

### 2.1 RGBT Tracking

RGBT tracking receives more and more attention in the computer vision community with the popularity of thermal infrared sensors. Recent methods on RGBT tracking mainly focus on sparse representation because of its capability of suppressing noise and errors [44], [26]. Wu *et al.* [44] concatenate the image patches from RGB and thermal sources into a one-dimensional vector that is then sparsely represented in the target template space. Collaborative sparse representation based trackers is proposed by Li *et al.* [26] to jointly optimize the sparse codes and modality weights online for more reliable tracking. And Li *et al.* [4] further consider heterogeneous property between different modalities and noise effects of initial seeds in the cross-modal ranking model. These methods rely on handcrafted features to track objects, and thus are difficult to handle the challenges of significant appearance changes caused by background clutter, deformation within each modality.

### 2.2 Feature Aggregation for Tracking

Feature aggregation [1, 47] is becoming more and more popular to improve network performance by enhancing the representation of

features. Without exception, in the field of visual tracking [6, 12, 15, 48], there are many methods to improve tracking performance by the skill of feature aggregation. Li *et al.* [6] design a FusionNet to directly aggregate RGB and thermal feature maps from the outputs of two-stream ConvNet. A aggregation of handcrafted low-level and hierarchical deep features is proposed by Danelljan *et al.* [12, 15] by employing an implicit interpolation model to pose the learning problem in the continuous spatial domain, which enable efficient integration of multi-resolution feature maps. Qi *et al.* [48] take full advantages of features from different CNN layers and used an adaptive Hedge method to hedge several CNN trackers into a stronger one. Li *et al.* [25] propose a new architecture to aggregate the middle to the deep layer features, which not only improves the accuracy but also reduces the model size. Different from these methods, we proposed a novel feature aggregation and pruning framework for RGBT tracking, which recursively aggregates all layer deep features while compressing feature channels.

### 3 PROPOSED APPROACH

In this section, we first describe the proposed training framework for RGBT object tracking. Then we introduce two modules of dense feature aggregation and feature pruning in detail.

#### 3.1 Network Architecture

As shown in Figure 2, the proposed network consists of a fully convolutional dense feature aggregation module, a feature pruning module and three fully connected layers(fc4-6) for binary classification. Following MDNet [36], we choose a lighter VGG-M network [40](conv1-3) as our backbone. Herein, two modalities adopt the same backbone network and share parameters. Different from original MDNet, max pooling layer is removed after conv2 layer, and dilated convolution with the rate as 3 is applied for extracting a dense feature map with a higher spatial resolution. Then we aggregate all features of two modalities by a feature aggregation block. To reduce feature noise interference, the aggregated features are selected by a feature pruning module. Finally, the optimized features are classified by three fully connected layers and softmax cross-entropy loss. The network has  $K$  branches (i.e. the  $K$  domains) which are denoted by the last fully connected layers, in other words, training sequences  $fc6^1 - fc6^K$ . More details of multi-domain learning can be found in [36].

#### 3.2 Dense Feature Aggregation

The dense feature aggregation module is a feature fusion strategy that aims at strengthening the fully convolutional architecture through parallel hierarchical structure. Its task is to better process and propagate the features from the original network to the classifier. Aggregation block, the main building blocks of the dense features aggregation module, learns to combine the output of multiple convolutional layers, and extract all spatial and semantic information from shallow to deep features. We implement the feature aggregation module as a parallel feature processing branch that can be plugged into any CNN architecture. Our aggregation consists of a stacking sequence of aggregation blocks, each one iteratively combining the output from the backbone and from the

previous aggregation block, as shown in Figure 2. When the inputs of a aggregation block have different scales, we use the max pooling operation to keep their sizes consistent. The proposed aggregation block are implemented as a  $1 \times 1$  convolution followed by non-linear(ReLU) and normalization(LRN) operations, as shown in Figure 2. Our structure can be combined with any existing pre-trained models without disrupting the propagation of the original features. To fully fuse features of different modalities, the outputs of RGB and thermal backbone network are all connected to the aggregation block. To map the features of the two modalities to the same feature space, we select the same backbone network and share the parameters. The dense feature aggregation module aggregates the spatial and semantic information of the two modalities from shallow to deep, and compresses the feature channels so that more rich and effective feature representation can be obtained. Let  $B(\cdot)$  denote the aggregation operation of the feature, and we have

$$B(\mathbf{x}_1, \dots, \mathbf{x}_n) = LRN(\sigma(\sum_i \mathbf{W}_i \mathbf{x}_i + \mathbf{b})), \quad i = 1, 2, \dots, n. \quad (1)$$

where  $\sigma$  is the non-linear activation, and  $\mathbf{W}_i$  and  $\mathbf{b}$  are the weights and bias in the convolution respectively. Local Response Normalization (LRN) is a normalized function, and  $\mathbf{x}$  denotes the input of a aggregation block.

#### 3.3 Feature Pruning

To eliminate noisy and redundant information introduced by the dense feature aggregation and inspired by [39], we propose a feature pruning mechanism. Note that our motivation is significantly different from [39]. [39] is a dropout technique to avoid overfitting, while we aim to prune out the redundant and noise features and retain the most discriminative features to a certain target for more effective localization, in addition to avoiding overfitting of network training. By this way, the learning of the effective feature representations is enhanced, and useless features are suppressed. In a specific, channel dropout [39] is used between two adjacent convolution layers, and the operations of Global Average Pooling (GAP), Weighted Random Selection (WRS) and Random Number Generation (RNG) are used to select some channels to achieve regularization. While our feature pruning operations will choose some channels with greater impact on target localization. If directly using [39] to achieve our goal, it would make our network difficult to optimize due to the dense aggregation structure of our network. In addition, the RNG operation would increase the randomness of feature selection and thus we leave out it.

Lin *et al.* [35] propose to replace the fully connected layer (FC) with GAP to solve the problem of overfitting and excessive FC layer parameters in convolutional neural networks. Zhou *et al.* [50] reveal that using GAP can make convolutional neural networks have excellent localization ability. Therefore, in this paper, we use GAP to obtain the activation state of each feature channel,

$$score_c = \frac{1}{W \times H} \sum_{j=1}^W \sum_{k=1}^H x_c(j, k) \quad (2)$$

where  $W$  and  $H$  are the width and height of feature map.  $x_c$  denotes the feature map of the  $c$ -th channel.

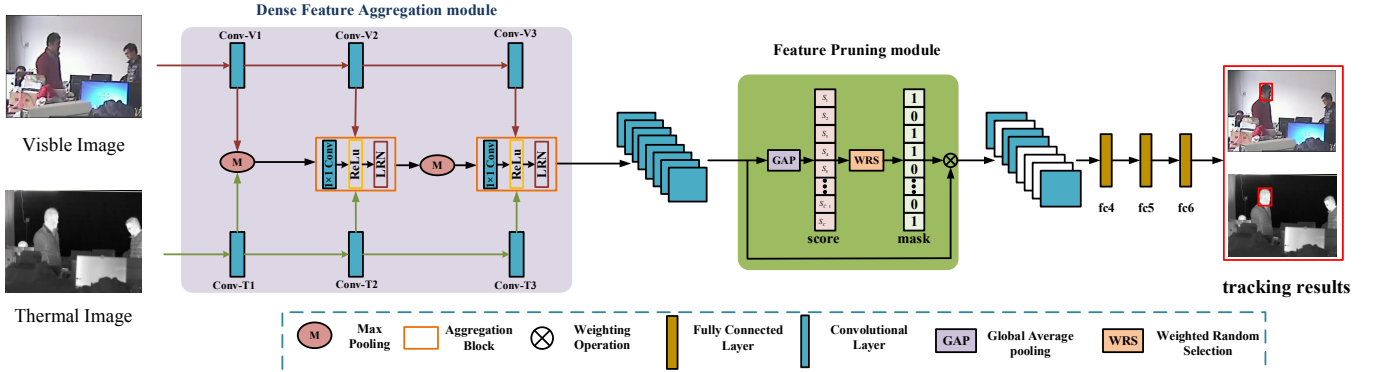


Figure 2: Diagram of the proposed network architecture. The network consists of two major modules, i.e., a dense feature aggregation module and a feature pruning module.

In this paper, we do not directly use the *score* to perform channel selection, but instead adopt WRS [16] which is a more efficient algorithm. Specifically, each channel  $x_c$  has  $score_c$ , a random number  $r_c \in (0, 1)$  is generated. The key value  $key_c$  is computed as

$$key_c = r_c^{\frac{1}{score_c}} \quad (3)$$

The  $M$  items of the largest key values are selected, where  $M = N * wrs\_ratio$ ,  $N$  is channels number and  $wrs\_ratio$  is a parameter indicating how many channels are selected after WRS. The detailed steps of the whole collaborative channel pruning can be found in Algorithm 1.

---

#### Algorithm 1 Feature Pruning.

---

**Input:**  
feature channel  $x_c$ , channel selection rate  $wrs\_ratio$ ;  
**Output:**  
1: Calculate channel  $score_c$  by Eq. 2;  
2: For each  $c$ ,  $r_c = random(0, 1)$  and calculate  $key_c$  value by Eq. 3;  
3: Select the  $M = N * wrs\_ratio$  items with the largest  $key_c$ ;  
4: Obtain the feature channels after feature pruning;  
5: **return**  $\tilde{x}_i$ ;

---

### 3.4 Network Training

In this section, we describe the training details of our network. First, we initialize the parameters of the first three convolutional layers using the pre-trained model of the VGG-M network [40]. While fully connected layers are initialized randomly. Then, we train the whole network by the Stochastic Gradient Descent (SGD) algorithm, where each domain is handled exclusively in each iteration. In each iteration, mini-batch is constructed from 8 frames which are randomly chosen in each video sequence. And we draw 32 positive and 96 negative samples from each frame which results in 256 positive and 768 negative data altogether in a mini-batch. The samples whose the IoU overlap ratios with the ground truth bounding box are larger than 0.7 are treated as positive, and the negative samples have less than 0.5. For multi-domain learning with  $K$  training sequences, we train the network with 100 epoch iterations by softmax cross-entropy loss. We train our network using

77 video sequences randomly selected from RGBT234 dataset [7] and test it on GTOT dataset [5]. For another experiment, we train our network on all 50 video sequences from GTOT dataset and test it on RGBT234 dataset.

### 3.5 Tracker Details

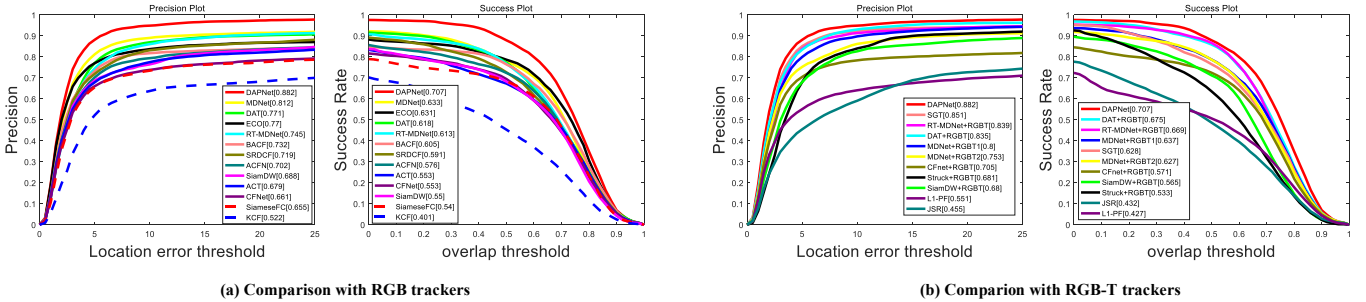
In tracking, the  $K$  branches of domain-specific layers (the last fc layer) are replaced with a single branch for each test sequence. Moreover, the feature pruning module is removed. During the tracking process and online fine-tuning, we fix the convolutional filters  $w_1, w_2, w_3$  and fine-tune the fully connected layers  $w_4, w_5, w_6$  because the convolutional layers would have generic tracking information whereas the fully-connected layers have the video-specific knowledge. Given the first frame pair with the ground truth of target object, we draw 500 positive (IoU with ground truth is larger than 0.7) and 5000 negative samples (IoU with ground truth is smaller than 0.5), and train the new branch with 10 iterations. Given the  $t$ -th frame, we draw a set of candidates  $\{z_t^i\}$  from a Gaussian distribution of the previous tracking result  $z_{t-1}^*$ , where the mean of Gaussian function is set to  $z_{t-1}^* = (a_{t-1}, b_{t-1}, s_{t-1})$  and the covariance is set as a diagonal matrix  $diag\{0.09r^2, 0.09r^2, 0.25\}$ .  $(a, b)$  and  $s$  indicate the location and scale respectively and  $r$  is the mean of  $(a_{t-1}, b_{t-1})$ . For the  $i$ -th candidate  $z_t^i$ , we compute its positive and negative scores using the trained network as  $f^+(z_t^i)$  and  $f^-(z_t^i)$ , respectively. The target location of the current frame is the candidate with the maximum positive score as:

$$z_t^* = \arg \max_{z_t^i} f^+(z_t^i), \quad i = 1, 2, \dots, N, \quad (4)$$

where  $N$  is the number of candidates. We also apply bounding box regression technique [37] to improve target localization accuracy. The bounding box regressor is trained only in the first frame to avoid potential unreliability of other frames. If the estimated target state is sufficiently reliable, i.e.  $f^+(z_t^*) > 0.5$ , we adjust the target locations using the regression model. More details can be referred to [37].

**Table 1: Attribute-based PR/SR scores (%) on RGBT234 dataset against with eight RGBT trackers. The best and second results are in red and green colors, respectively.**

	SOWP+RGBT	CFNet+RGBT	KCF+RGBT	L1-PF	CSR-DCF+RGBT	MEEM+RGBT	SGT	MDNet+RGBT1	DAPNet
NO	86.8/53.7	76.4/56.3	57.1/37.1	56.5/37.9	82.6/60.0	74.1/47.4	<b>87.7</b> /55.5	86.2/ <b>61.1</b>	<b>90.0</b> / <b>64.4</b>
PO	74.7/48.4	59.7/41.7	52.6/34.4	47.5/31.4	73.7/ <b>52.2</b>	68.3/42.9	<b>77.9</b> /51.3	76.1/51.8	<b>82.1</b> / <b>57.4</b>
HO	57.0/37.9	41.7/29.0	35.6/23.9	33.2/22.2	59.3/40.9	54.0/34.9	59.2/39.4	<b>61.9</b> / <b>42.1</b>	<b>66.0</b> / <b>45.7</b>
LI	<b>72.3</b> /46.8	52.3/36.9	51.8/34.0	40.1/26.0	69.1/ <b>47.4</b>	67.1/42.1	70.5/46.2	67.0/45.5	<b>77.5</b> / <b>53.0</b>
LR	72.5/46.2	55.1/36.5	49.2/31.3	46.9/27.4	72.0/47.6	60.8/37.3	<b>75.1</b> /47.6	<b>75.9</b> / <b>51.5</b>	75.0/ <b>51.0</b>
TC	70.1/44.2	45.7/32.7	38.7/25.0	37.5/23.8	66.8/46.2	61.2/40.8	<b>76.0</b> / <b>47.0</b>	75.6/ <b>51.7</b>	<b>76.8</b> / <b>54.3</b>
DEF	65.0/46.0	52.3/36.7	41.0/29.6	36.4/24.4	63.0/46.2	61.7/41.3	<b>68.5</b> / <b>47.4</b>	66.8/47.3	<b>71.7</b> / <b>51.8</b>
FM	63.7/38.7	37.6/25.0	37.9/22.3	32.0/19.6	52.9/35.8	59.7/36.5	<b>67.7</b> / <b>40.2</b>	58.6/36.3	<b>67.0</b> / <b>44.3</b>
SV	66.4/40.4	59.8/43.3	44.1/28.7	45.5/30.6	70.7/49.9	61.6/37.6	69.2/43.4	<b>73.5</b> / <b>50.5</b>	<b>78.0</b> / <b>54.2</b>
MB	63.9/42.1	35.7/27.1	32.3/22.1	28.6/20.6	58.0/42.5	55.1/36.7	64.7/43.6	<b>65.4</b> / <b>46.3</b>	<b>65.3</b> / <b>46.7</b>
CM	65.2/43.0	41.7/31.8	40.1/27.8	31.6/22.5	61.1/44.5	58.5/38.3	<b>66.7</b> / <b>45.2</b>	64.0/ <b>45.4</b>	<b>66.8</b> / <b>47.4</b>
BC	64.7/41.9	46.3/30.8	42.9/27.5	34.2/22.0	61.8/41.0	62.9/38.3	<b>65.8</b> /41.8	64.4/ <b>43.2</b>	<b>71.7</b> / <b>48.4</b>
ALL	69.6/45.1	55.1/39.0	46.3/30.5	43.1/28.7	69.5/49.0	63.6/40.5	72.0/47.2	<b>72.2</b> / <b>49.5</b>	<b>76.6</b> / <b>53.7</b>



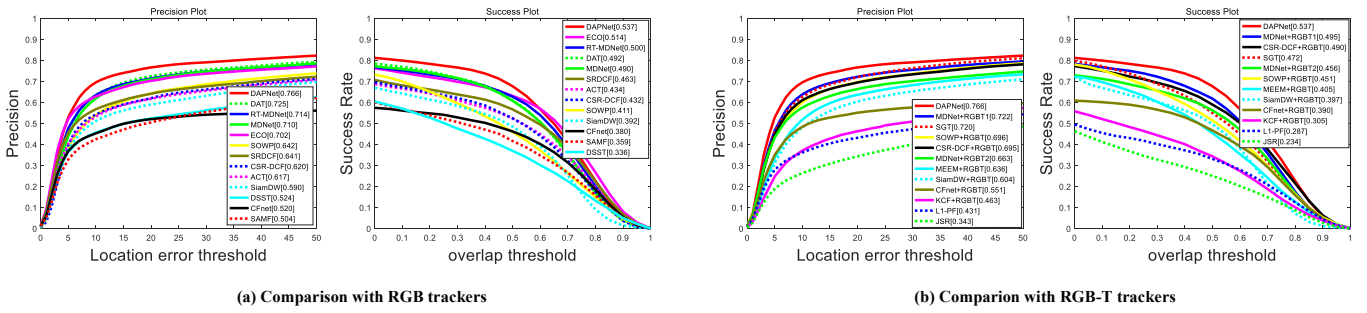


**Figure 4: Evaluation curves on RGBT234 dataset. The representative scores of PR/SR are presented in the legend. For clarity, we separate RGB and RGBT trackers in (a) and (b) respectively.**

**Table 2: Performance of our method against MDNet with different implementation strategies on GTOT and RGBT234 datasets.**

		MDNet	MDNet+RGBT1	MDNet+RGBT2	DAPNet
GTOT	PR	81.2	80.0	75.3	88.2
	SR	63.3	63.7	62.7	70.7
RGBT234	PR	71.0	72.2	66.3	76.6
	SR	49.0	49.5	45.6	53.7

lower than MDNet. There are two possible reasons. 1) Directly concatenating two modal data does not make effective use of complementary information between modalities. 2) Redundant features and noise interference might be introduced. These validate that the direct and simple concatenate of two modal data does not achieve good tracking performance, and also verify the effectiveness of our dense feature aggregation and pruning.

## 4.2 Evaluation on GTOT

**Comparison with RGB trackers.** To verify the superiority of the proposed RGBT tracking method compared to RGB tracking, we first evaluate our method with twelve state-of-the-art RGB tracker, including DAT [38], RT-MDNet [22], SiamDW [49], ACT [3], MDNet [37], ECO [12], BACF [17], SRDCF [14], ACFN [8], SiameseFC [2], CFnet [43] and KCF [19]. Figure 3(a) shows that our method outperforms these trackers, demonstrating the effectiveness of introducing thermal information in visual tracking. In particular, our tracker outperforms MDNet and DAT with 7.0%/7.4%, 11.1%/8.9% in PR/SR, respectively.

**Comparison with RGBT trackers.** We further compare our tracker with several state-of-the-art RGBT trackers, including RT-MDNet+RGBT, DAT+RGBT, SiamDW+RGBT, CSR [5], JSR [41], L1-PF [45], SGT [30], MDNet+RGBT1, and MDNet+RGBT2. Since there are few RGBT trackers [26, 27, 30, 33], some RGB tracking methods have been extended to RGB-T ones by concatenating RGB and thermal features into a single vector or regarding the thermal as an extra channel, such as RT-MDNet, DAT, SiamDW and CFnet. Figure 3(b) shows that our tracker significantly outperforms them, demonstrating the effectiveness of employing RGB and thermal information adaptively to construct robust feature representations in our approach. In particular, our tracker achieves 3.1%/7.9% and 4.3%/3.8% performance gains in PR/SR over SGT and RT-MDNet+RGBT.

**Table 3: Evaluation results of our DAPNet with its variants on RGBT234 dataset.**

		DAPNet-noFACP	DAPNet-noFA	DAPNet-noFP	DAPNet
RGBT234	PR	66.3	67.0	74.3	76.6
	SR	45.6	47.1	52.5	53.7

## 4.3 Evaluation on RGBT234

For more comprehensive evaluation, we report the evaluation results on the RGBT234 dataset [7], as shown in Figure 4. The comparison trackers include twelve RGB ones (DAT [38], RT-MDNet [22], SiamDW [49], ACT [3], MDNet [37], ECO [12], SOWP [23], SRDCF [14], CSR-DCF [34], DSST [13], CFnet [43] and SAMF [46]) and eleven RGBT ones (MDNet+RGBT1, MDNet+RGBT2, SGT [30], SOWP+RGBT, CSR-DCF+RGBT, MEEM [21]+RGBT, CFnet+RGBT, KCF [19]+RGBT, JSR [41] and L1-PF [45]). From the results, we can see that the performance of our method clearly outperforms the state-of-the-art RGB and RGBT methods in all metrics. It demonstrates the importance of thermal information and our method. In particular, our method achieves 4.1%/4.5% performance gains in PR/SR over the second best RGB tracker DAT, and achieves 4.4%/4.2% and 4.6%/6.5% gains over MDNet+RGBT1 and SGT, respectively. Note that the methods based on Siamese network [9] have weak performance on RGBT234 and GTOT, including SiamDW, CFNet and SiameseFC. It is because of the great gap between the training datasets and the test datasets (RGBT234 and GTOT), and those methods might only fit the training dataset very well but the test results are poor.

**Attribute-based performance.** We also report the attribute-based results of our method versus other state-of-the-art RGBT trackers on RGBT234 dataset, including L1-PF, KCF+RGBT, MEEM+RGBT, SOWP+RGBT, CSR-DCF+RGBT, CFNet+RGBT, SGT and MDNet+RGBT1, as shown in Table 1. The attributes include no occlusion (NO), partial occlusion (PO), heavy occlusion (HO), low illumination (LI), low resolution (LR), thermal crossover (TC), deformation (DEF), fast motion (FM), scale variation (SV), motion blur (MB), camera moving (CM) and background clutter (BC). The results show that our method performs the best in terms of most challenges except for NO, PO, LI, BC, and SV. It demonstrates the effectiveness of our method in handling the sequences with the appearance changes and adverse conditions.

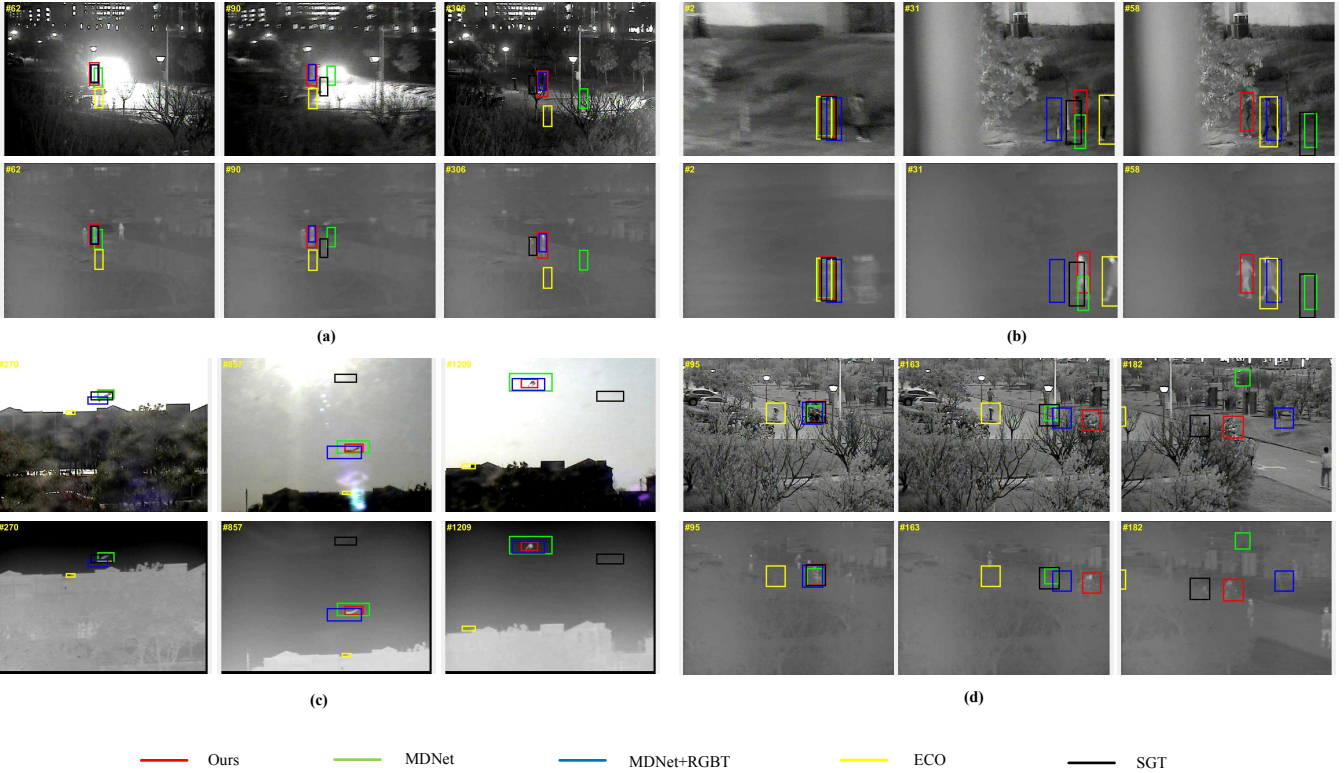


Figure 5: Visual comparison of our DAPNet versus four state-of-the-art trackers on four video sequences.

#### 4.4 Ablation Study

To justify the significance of the main components using RGBT234, we implement 3 special versions of our approach for comparative analysis including, 1) DAPNet-noFACP, that removes the dense feature aggregation and feature pruning, which is MDNet+RGBT2. 2) DAPNet-noFA, that removes the dense feature aggregation and only use feature pruning. 3) DAPNet-noFP, that removes the feature pruning and only use dense feature aggregation. From Table 3 we can see that, 1) Introducing the dense feature aggregation has a big performance boost by observing DAPNet-noFP against DAPNet-noFACP. 2) DAPNet-noFA is better than DAPNet-noFACP, and the similar observation can be obtained for DAPNet with DAPNet-noFP. It suggests that the feature pruning scheme could handle noise interference, and thus lead to tracking performance improvement. 3) DAPNet outperforms DAPNet-noFACP, DAPNet-noFA and DAPNet-noFP, which justify the effectiveness of the whole framework with the dense feature aggregation and feature pruning.

#### 4.5 Qualitative Performance

The qualitative comparison of our algorithm versus two state-of-the-art RGB trackers and two state-of-the-art RGBT trackers on partial video sequences is presented in Figure 5, including MDNet [36], ECO [12], MDNet+RGBT2 and SGT [30]. Our approach shows consistently better performance in various challenging scenarios including high illumination, motion blur, scale variation and background clutter. For example, in Figure 5 (a), the *man* is

totally invisible in RGB source but the thermal images can provide reliable information to distinguish the target from the background. In Figure 5(d), our method performs well in presence of partial occlusions and background clutter while other trackers lose the target. Compared with four trackers, the superiority of our tracker is fully demonstrated in these extreme challenges. It also verifies that dense feature aggregation and pruning can enhance image features to obtain better tracking results.

## 5 CONCLUSION

We have proposed an end-to-end deep network for RGBT tracking. Our network consists of two major modules, one is dense feature aggregation that provides a powerful RGBT feature representations for target objects, and another is feature pruning that collaboratively select most discriminative feature maps from two modalities for enhancement of RGBT features. Extensive experiments on two benchmark datasets demonstrate that our approach is able to handle various challenges like background clutter and partial occlusion, and thus improves tracking performance significantly. In future work, we will investigate a wider and deeper network [49] in our framework to further boost RGBT tracking performance, and improve the network structure (i.e., [22] extract more accurate representations of targets and candidates by RoIAlign ) to achieve real-time performance.

## ACKNOWLEDGMENTS

This research is jointly supported by the National Natural Science Foundation of China (No. 61860206004, 61702002, 61872005), Natural Science Foundation of Anhui Province (1808085QF187), Open fund for Discipline Construction, Institute of Physical Science and Information Technology, Anhui University.

## REFERENCES

- [1] D’Innocente Antonio and Caputo Barbara. 2018. Domain Generalization with Domain-Specific Aggregation Modules. *arXiv: 1809.10966* (2018).
- [2] Luca Bertinetto, Jack Valmadre, Joāo F. Henriques, Andrea Vedaldi, and Philip H. S. Torr. 2016. Fully-Convolutional Siamese Networks for Object Tracking. In *European Conference on Computer Vision*.
- [3] Chen Boyu, Wang Dong, Li Peixia, Wang Shuang, and Lu Huchuan. 2018. Real-time Actor-Critic Tracking. In *the European Conference on Computer Vision*.
- [4] Li Chenglong, Zhu Chengli, Huang Yan, Tang Jin, and Wang Liang. 2018. Cross-modal ranking with soft consistency and noisy labels for robust RGB-T tracking. In *Proceedings of European Conference on Computer Vision*.
- [5] Li Chenglong, Cheng Hui, Shiyi. Hu, Liu Xiaobai, Tang Jin, and Lin Liang. 2016. Learning Collaborative Sparse Representation for Grayscale-thermal Tracking. *IEEE Transactions on Image Processing* 25, 12 (2016), 5743–5756.
- [6] Li Chenglong, Wu Xiaohao, Zhao Nan, Cao Xiaochun, and Tang Jin. 2018. Fusing Two-Stream Convolutional Neural Networks for RGB-T Object Tracking. *IEEE Transactions on Information Theory* 281 (2018), 78–85.
- [7] Li Chenglong, Liang Xinyan, Lu Yijuan, Zhao Nan, and Tang Jin. 2019. RGB-T object tracking: benchmark and baseline. *Pattern Recognition* (2019), 106977.
- [8] Jongwon Choi, Hyung Jin Chang, Sangdoo Yun, Tobias Fischer, and Young Choi Jin. 2017. Attentional Correlation Filter Network for Adaptive Visual Tracking. In *IEEE Conference on Computer Vision and Pattern Recognition*.
- [9] Sumit Chopra, Raia Hadsell, Yann LeCun, et al. 2005. Learning a similarity metric discriminatively, with application to face verification. In *IEEE Conference on Computer Vision and Pattern Recognition*.
- [10] Ciaran O Conaire, Noel E. Connor, and Alan Smeaton. 2007. Thermo-visual feature fusion for object tracking using multiple spatiogram trackers. *Machine Vision and Applications* 7 (2007), 1–12.
- [11] Ciarān ÅŞ Conaire, Noel E. O’Connor, Eddie Cooke, and Alan F. Smeaton. 2006. Comparison of fusion methods for thermo-visual surveillance tracking. In *International Conference on Information Fusion*.
- [12] M. Danelljan, G. Bhat, F. S. Khan, and M. Felsberg. 2017. ECO: Efficient Convolution Operators for Tracking. In *Proceedings of IEEE Conference on Computer Vision and Pattern Recognition*.
- [13] Martin Danelljan, Gustav Häger, Fahad Khan, and Michael Felsberg. 2014. Accurate scale estimation for robust visual tracking. In *Proceedings of British Machine Vision Conference*.
- [14] Martin Danelljan, Gustav Häger, Fahad Shahbaz Khan, and Michael Felsberg. 2015. Learning spatially regularized correlation filters for visual tracking. In *the IEEE International Conference on Computer Vision*.
- [15] Martin Danelljan, Andreas Robinson, Fahad Shahbaz Khan, and Michael Felsberg. 2016. Beyond correlation filters: Learning continuous convolution operators for visual tracking. In *European Conference on Computer Vision*.
- [16] Pavlos S. Efraimidis and Paul G. Spirakis. 2006. Weighted random sampling with a reservoir. *Inform. Process. Lett.* 97, 5 (2006), 181–185.
- [17] Hamed Kiani Galoogahi, Ashton Fagg, and Simon Lucey. 2017. Learning Background-Aware Correlation Filters for Visual Tracking. In *IEEE International Conference on Computer Vision*.
- [18] Yihui He, Xiangyu Zhang, and Sun Jian. 2017. Channel Pruning for Accelerating Very Deep Neural Networks. (2017).
- [19] J. F. Henriques, R Caseiro, P Martins, and J Batista. 2015. High-Speed Tracking with Kernelized Correlation Filters. *IEEE Transactions on Pattern Analysis and Machine Intelligence* 37, 3 (2015), 583–596.
- [20] Luo Jianhao, Wu Jianxin, and Lin Weiyao. 2017. Thinet: A filter level pruning method for deep neural network compression. In *the IEEE international conference on computer vision*.
- [21] Zhang Jianming, Ma Shugao, and Stan. Sclaroff. 2014. MEEM: robust tracking via multiple experts using entropy minimization. In *European Conference on Computer Vision*.
- [22] Ilchae Jung, Jeany Son, Mooyeon Baek, and Bohyung Han. 2018. Real-Time MDNet. In *European Conference on Computer Vision*.
- [23] Han Ul Kim, Dae Youn Lee, Jee Young Sim, and Chang Su Kim. 2015. SOWP: Spatially Ordered and Weighted Patch Descriptor for Visual Tracking. In *IEEE International Conference on Computer Vision*.
- [24] Xiangyuan Lan, Mang Ye, Shengping Zhang, and Pong C. Yuen. 2018. Robust Collaborative Discriminative Learning for RGB-Infrared Tracking. In *Proceedings of the AAAI Conference on Artificial Intelligence*.
- [25] Bo Li, Wei Wu, Qiang Wang, Fangyi Zhang, and Junjie Yan. 2019. SiamRPN++: Evolution of Siamese Visual Tracking with Very Deep Networks. In *IEEE Conference on Computer Vision and Pattern Recognition*.
- [26] C. Li, H. Cheng, S. Hu, X. Liu, J. Tang, and L. Lin. 2016. Learning Collaborative Sparse Representation for Grayscale-Thermal Tracking. *IEEE Transactions on Image Processing* 25, 12 (2016), 5743–5756.
- [27] Chenglong Li, Hu Shiyi, Gao Sihan, and Tang Jin. 2016. Real-time grayscale-thermal tracking via Laplacian sparse representation. In *Proceedings of International Conference on Multimedia Modeling*.
- [28] C. Li, X. Sun, X. Wang, L. Zhang, and J. Tang. 2017. Grayscale-thermal Object Tracking via Multi-task Laplacian Sparse Representation. *IEEE Transactions on Systems, Man, and Cybernetics: Systems* 47, 4 (2017), 673–681.
- [29] Chenglong Li, Xiaohao Wu, Zhiimin Bao, and Jin Tang. 2017. ReGLE: spatially regularized graph learning for visual tracking. In *the 25th ACM international conference on Multimedia*.
- [30] Chenglong Li, Nan Zhao, Yijuan Lu, Chengli Zhu, and Jin Tang. 2017. Weighted Sparse Representation Regularized Graph Learning for RGB-T Object Tracking. In *Proceedings of ACM International Conference on Multimedia*.
- [31] Chenglong Li, Chengli Zhu, Jian Zhang, Bin Luo, and Jin Tang. 2018. Learning Local-Global Multi-Graph Descriptors for RGB-T Object Tracking. *IEEE Transactions on Circuits and Systems for Video Technology* PP, 99 (2018), 1–1.
- [32] Xin Li, Chao Ma, Baoyuan Wu, Zhenyu He, and Ming-Hsuan Yang. 2019. Target-Aware Deep Tracking. (2019).
- [33] Huaping Liu and Fuchun Sun. 2012. Fusion tracking in color and infrared images using joint sparse representation. *Information Sciences* 55, 3 (2012), 590–599.
- [34] A. Lukezic, T. Vojir, L. C. Zajc, J. Matas, and M. Kristan. 2016. Discriminative correlation filter with channel and spatial reliability. In *IEEE Conference on Computer Vision and Pattern Recognition*.
- [35] Lin Min, Chen Qiang, and Shuicheng Yan. 2013. Network In Network. *Computer Science* (2013).
- [36] Hyeonseob Nam and Bohyung Han. 2015. Learning Multi-Domain Convolutional Neural Networks for Visual Tracking. In *IEEE Conference on Computer Vision and Pattern Recognition*.
- [37] Hyeonseob Nam and Bohyung Han. 2016. Learning Multi-Domain Convolutional Neural Networks for Visual Tracking. In *IEEE Conference on Computer Vision and Pattern Recognition*.
- [38] Shi Pu, Yibing Song, Chao Ma, Honggang Zhang, and Ming Hsuan Yang. 2018. Deep Attentive Tracking via Reciprocal Learning. In *Advances in Neural Information Processing Systems*.
- [39] Hou Saihui and Wang Zilei. 2019. Weighted Channel Dropout for Regularization of Deep Convolutional Neural Network. In *AAAI Conference on Artificial Intelligence*.
- [40] Karen Simonyan and Andrew Zisserman. 2015. Very deep convolutional networks for large-scale image recognition. In *International Conference on Learning Representations*.
- [41] Fuchun Sun and Huaping Liu. 2012. Fusion tracking in color and infrared images using joint sparse representation. *Science China Information Sciences* 55, 3 (2012), 590–599.
- [42] Kong Tao, Anbang Yao, Yurong Chen, and Fuchun Sun. 2016. HyperNet: Towards Accurate Region Proposal Generation and Joint Object Detection. In *IEEE Conference on Computer Vision and Pattern Recognition*.
- [43] Jack Valmadre, Luca Bertinetto, Joāo F. Henriques, Andrea Vedaldi, and Philip H. S. Torr. 2017. End-To-End Representation Learning for Correlation Filter Based Tracking. In *IEEE Conference on Computer Vision and Pattern Recognition*.
- [44] Yi Wu, E. Blasch, Genshe Chen, Li Bai, and Haibin Ling. 2011. Multiple source data fusion via sparse representation for robust visual tracking. In *International Conference on Information Fusion*.
- [45] Yi Wu, Erik Blasch, Genshe Chen, Li Bai, and Haibing Ling. 2011. Multiple source data fusion via sparse representation for robust visual tracking. In *International Conference on Information Fusion*.
- [46] Li Yang and Jianmei Zhu. 2014. A Scale Adaptive Kernel Correlation Filter Tracker with Feature Integration. In *Proceedings of European Conference on Computer Vision*.
- [47] Fisher Yu, Dequan Wang, Evan Shelhamer, and Trevor Darrell. 2018. Deep Layer Aggregation. (2018).
- [48] Qi Yuankai, Zhang Shengping, Qin Lei, Yao Hongxun, Huang Qingming, Lim Jongwoo, and Yang Ming-Hsuan. 2016. Hedged Deep Tracking. In *IEEE Conference on Computer Vision and Pattern Recognition*.
- [49] Zhang Zhipeng, Peng Houwen, and Wang Qiang. 2019. Deeper and Wider Siamese Networks for Real-Time Visual Tracking. In *Proceedings of IEEE Conference on Computer Vision and Pattern Recognition*.
- [50] Bolei Zhou, Aditya Khosla, Agata Lapedriza, Aude Oliva, and Antonio Torralba. 2016. Learning Deep Features for Discriminative Localization. In *IEEE Conference on Computer Vision and Pattern Recognition*.